

## Structural and Infrared Studies of Zn-Ti Substituted $MgZn_xTi_xFe_{2-2x}O_4$ Ferrite Prepared via Solid State Reaction Technique

\*S.V. Kshirsagar

\*Department of Physics, Mrs. K.S.K. Alias Kaku Arts, Science and Commerce College, Beed. Dist. Beed Maharashtra (India)

\*Corresponding author: [kshiva\\_pvp@rediffmail.com](mailto:kshiva_pvp@rediffmail.com)

### Abstract

The samples of  $MgZn_xTi_xFe_{2-2x}O_4$  spinel ferrite systems with varying  $x$  [ $x = 0.0, 0.1, 0.2, 0.3, 0.4, 0.5$  and  $0.6$ ] were synthesized by double sintering solid state reaction method. A.R. grade oxides of magnesium, zinc, titanium and ferric were used for the preparation of ferrite system and all the synthesized powder samples were characterized at room temperature by using X-ray diffraction pattern. The X-ray diffraction patterns were recorded in the  $2\theta$  range of  $20^\circ$ - $80^\circ$  using  $Cu-K\alpha$  radiation. The analysis of X-ray diffraction patterns revealed the formation of single-phase cubic spinel structure. The lattice constant increases with Zn, Ti concentration 'x'. The X-ray density decreases with increase in Zn, Ti concentration 'x'. The values of bulk density increase with Ti and Zn ions and porosity values varies in between 36% - 48%. The average particle size of all sample showed good agreement with the reported data and the values of hopping length, tetrahedral and octahedral bond length ( $d_{Ax}$ ) and ( $d_{Bx}$ ), shared tetrahedral and octahedral edge shows same behavior that of lattice constant. The Infrared (IR) spectra study shows two prominent absorption bands is recorded at room temperature associated with intrinsic vibration of the tetrahedral complexes for high frequency and for low frequency bands associated with octahedral complexes. Debye temperature obtained from IR data increases with composition 'x'.

**Keywords:** Spinel ferrite, Lattice constant, XRD, Infrared spectra, Debye temperature.

### 1. Introduction

Magnetic particles of mixed spinel ferrites have been the subject of current interest because of their interesting magnetic, electric, dielectric and optical properties. Technological advances in a variety of areas have generated a growing demand for the research and application of magnetic materials such as ferrites in devices [1-3]. Ferrites have many applications in high frequency devices, and they play a useful role in technological and magnetic applications because of their high electrical resistivity and sufficiently low dielectric losses over a wide range of frequencies. The first use of ferrite materials in a power application was to provide the time dependent magnetic deflection of the electron beam in the television receivers where the two

ferrite components use where the deflection yoke and flyback transformer. For many applications of soft ferrites, the absorption of energy due to the onset of ferromagnetic resonance was determined. These properties form the basis of the technologies of space telecommunication and radar. Frequently, ferrites are the only materials available for these applications [4].

The general chemical formula of ferrite possessing the structure of the mineral spinel,  $MgAl_2O_4$  is  $MFe_2O_4$ . The presence of  $Fe^{3+}$ ,  $Fe^{2+}$ ,  $Ni^{2+}$  and  $Mn^{2+}$  can be used to provide the unpaired electron spins. Other divalent ions such as  $Mg^{2+}$  or  $Zn^{2+}$  (or monovalent ions such as  $Li^+$ ) are not paramagnetic but affect the  $Fe^{3+}$  ions on the crystal lattice sites to provide or increase the magnetic moment.

Among titanium oxides of spinel structures, magnesium titanates are closely related to  $\text{LiTi}_2\text{O}_4$ , because the ionic radius of  $\text{Mg}^{2+}$  (0.86 Å) is quite close to that of  $\text{Li}^+$  (0.86 Å) [5,6]. The compound  $\text{MgFe}_2\text{O}_4$  is a partly inverted spinel ( $x = 1/3$  and  $y = 2/3$ ), which behaves as a collinear ferrimagnet. When the B sites are diluted by Ti, according to the Monte-Carlo simulation of Scoll and Binder [7], it has been observed that the electrical resistivity is markedly changed by controlling the firing temperature, atmosphere, and appropriate type and amount of substituent [8,9]. The  $(\text{Fe}_x\text{Mg}_{1-x})(\text{Fe}_{2y}\text{Mg}_{2-2y}\text{Ti}_i)\text{O}_4$  system was already studied by magnetic and Mössbauer measurements [10]. An understanding of mechanism involved in the changes brought about by the addition of substituent provides useful information for specific application. Abbas et al. [11] studied  $\text{Mg}_{x+1}\text{Ti}_x\text{Fe}_{2-2x}\text{O}_4$  ferrite and found that the compound has a spinel structure. Joshi et al [12] studied the Zn substituted  $\text{MgFe}_2\text{O}_4$  and found the interesting results on susceptibility, magnetization and Mössbauer. The combined effect of Zn and Ti on the properties of Mg ferrite is not reported in the literature. In the present paper, the structural and Infrared spectra studies of  $\text{MgZn}_x\text{Ti}_x\text{Fe}_{2-2x}\text{O}_4$  ferrite were carried out to discuss the role of  $\text{Ti}^{4+}$  and  $\text{Zn}^{2+}$  ions substitution.

## 2. Experimental Details

The samples of  $\text{MgZn}_x\text{Ti}_x\text{Fe}_{2-2x}\text{O}_4$  spinel ferrite systems with varying x [x = 0.0, 0.1, 0.2, 0.3, 0.4, 0.5 and 0.6] were synthesized by double sintering solid state reaction method. AR grade oxides of magnesium, zinc, titanate and ferric were used for the preparation of  $\text{MgZn}_x\text{Ti}_x\text{Fe}_{2-2x}\text{O}_4$  ferrite. The presintering and final sintering of the samples was carried out at temperature  $950^\circ\text{C}$  (12 hours) and  $1100^\circ\text{C}$  (12 hours) respectively. The sintered samples in the form of

pellet were furnace cooled to room temperature. The powder X-ray diffraction technique has been employed in the present study to characterize the samples of  $\text{MgZn}_x\text{Ti}_x\text{Fe}_{2-2x}\text{O}_4$  at room temperature. The X-ray diffraction (XRD) patterns were recorded in the  $2\theta$  range of  $20^\circ$ - $80^\circ$  using  $\text{Cu-K}\alpha$  radiation at room temperature.

The infrared (IR) spectral data for all samples was collected using Perkin Elmer spectrophotometer in the wave number ranges from  $200\text{ cm}^{-1}$  to  $800\text{ cm}^{-1}$ .

## 3. Results and Discussion

### 3.1. X-Ray diffraction study

Room temperature X-ray diffraction patterns typical samples, x = 0.1, 0.2, 0.3 of the  $\text{MgZn}_x\text{Ti}_x\text{Fe}_{2-2x}\text{O}_4$  system are depicted in **Fig.1**.

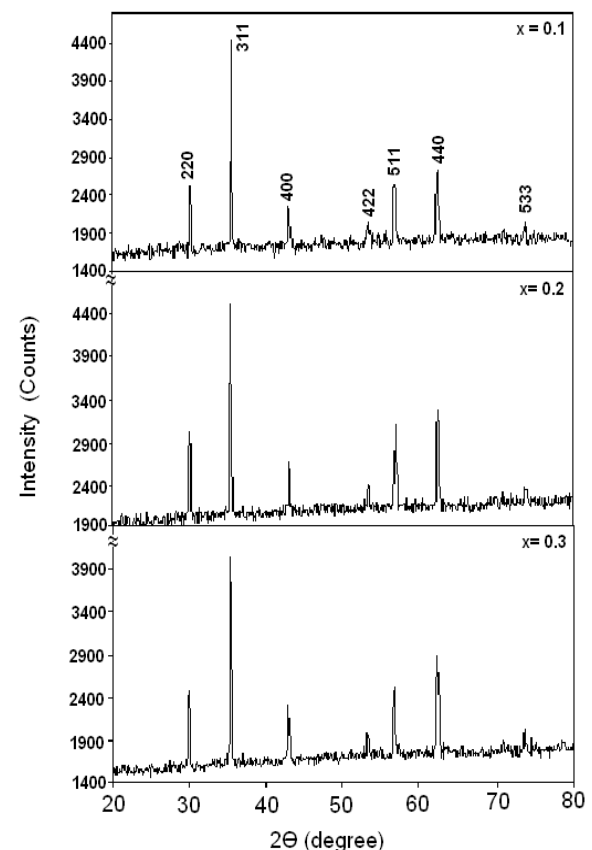


**Fig. 1:** X-ray diffraction (XRD) patterns for the typical samples, x = 0.1, 0.2, and 0.3 of the  $\text{MgZn}_x\text{Ti}_x\text{Fe}_{2-2x}\text{O}_4$  system

All the XRD patterns are clean and do not contain any impurity phase. No extra peak was obtained in this pattern. All the peaks in the XRD patterns are assigned by the (hkl) values. The XRD pattern clearly shows the presence of (220), (311), (222), (400), (422), (511), (440), (533).

All these reflections belong to cubic spinel structure. All these peaks shift towards right side due to substitution of Zn and Ti ions [13]. This is confirmed by the change in the interplanar spacing values. The interplanar spacing values are as listed in the following **Table 1**.

**Table 1:** Miller indices, and interplanar spacing (d) of  $MgZn_xTi_xFe_{2-2x}O_4$  system

Plane	Interplanar spacing (d) Å						
	0.0	0.1	0.2	0.3	0.4	0.5	0.6
(220)	2.970	2.970	2.980	2.980	2.980	2.980	2.989
(311)	2.537	2.537	2.537	2.544	2.544	2.543	2.544
(222)	2.418	2.463	2.431	2.437	2.418	2.437	2.443
(400)	2.100	2.104	2.104	2.109	2.109	2.109	2.109
(422)	1.713	1.716	1.717	2.720	1.722	1.722	2.722
(511)	1.616	1.619	1.621	1.621	1.624	1.624	1.624
(440)	1.484	1.487	1.488	1.491	1.493	1.493	1.493
(533)	1.277	1.283	1.284	1.286	1.287	1.287	1.287

The interplanar spacing (d) values were calculated for the reflection peaks using Bragg's law and the lattice constant 'a' was calculated. It is the distance between two adjacent planes of the crystal. It is different for different substances. For the present system samples, it is found that

the lattice parameter increases with increasing Zn and Ti ions substitution. The values of Miller indices and interplanar spacing 'd' are used to determine lattice constant 'a' of the spinel ferrite system and the values of lattice constant are given in **Table 2**.

**Table 2:** Lattice constant (a), X-ray density (dx), bulk density (d), porosity (P) and particle size (t) of the  $MgZn_xTi_xFe_{2-2x}O_4$  system

Comp. x	Lattice constant 'a' (Å)	X-ray density 'dx' (gm/cm <sup>3</sup> )	Bulk density 'd' (gm/cm <sup>3</sup> )	Porosity 'P' %	Particle Size 't' (Å)
0.0	8.37	4.492	2.823	41.59	278.77
0.1	8.39	4.447	2.633	36.29	279.69
0.2	8.40	4.445	2.374	46.65	318.12
0.3	8.42	4.442	2.371	46.55	303.13
0.4	8.43	4.437	2.328	47.52	301.43
0.5	8.45	4.439	2.305	48.06	306.23
0.6	8.46	4.432	2.267	48.84	295.63

The lattice constant increases with co-substitution of Zn and Ti ions. The linear increase in lattice constant with composition 'x' is depicted in the **Fig. 2**.

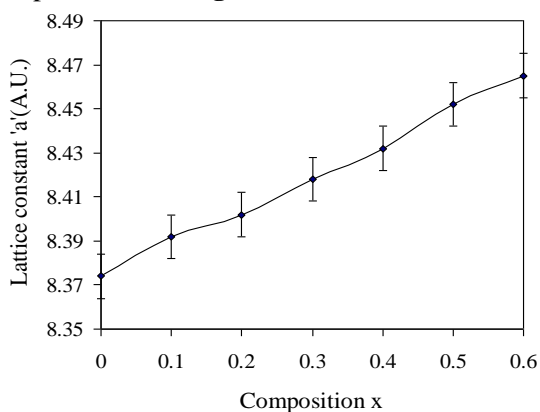


**Fig. 2:** Lattice constant of the system  $MgZn_xTi_xFe_{2-2x}O_4$  for  $x=0.0-0.6$ .

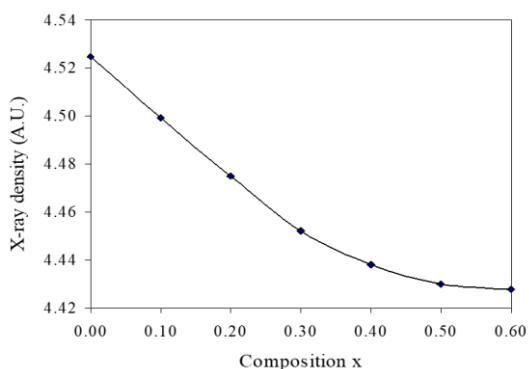


**Fig. 3** X-ray density (dx) of the system  $MgZn_xTi_xFe_{2-2x}O_4$  for  $x=0.0-0.6$ .

In the present series of  $MgZn_xTi_xFe_{2-2x}O_4$ ,  $2Fe^{3+}$  ions are replaced by combinations of divalent  $Zn^{2+}$  ions and tetravalent  $Ti^{4+}$  ions. The average ionic radii of  $Zn^{2+}$  and  $Ti^{4+}$  is quite large than that of  $Fe^{3+}$  ions and hence the substitution of Zn, Ti ions in place of  $Fe^{3+}$  ions cause the increase in lattice constant of the system

$MgZn_xTi_xFe_{2-2x}O_4$ . In Zn substituted  $MgFe_2O_4$  lattice constant increases with Zn substitution. Similarly in Ti substituted  $MgFe_2O_4$  lattice constant increases. With co-substitution of Zn and Ti the lattice constant of the  $MgFe_2O_4$  spinel ferrite also increases [14].

The X-ray density 'dx' for all the composition x was calculated by using the values of lattice constant 'a' and molecular weight of each sample. The values of X-ray density are given **Table 2**. Density plays a key role in controlling the properties of polycrystalline ferrites. The X-ray density decreases from the values of  $x=0.0$  to  $0.2$  and then slightly increases with increase in composition x. The variation of X-ray density with composition x is shown in the **Fig. 3**.

The bulk density of all the samples of the ferrite system  $MgZn_xTi_xFe_{2-2x}O_4$  was determined using the values of mass and volume of the samples. The values of bulk density are given in **Table 2**. The bulk density decreases with the substitution of Zn, Ti ions.

The X-ray density dx for all the samples was calculated using the values of molecular weight and lattice constant of the system. The values of X-ray density are given in **Table 2**. Like bulk density, X-ray density also decreases with the substitution of Zn, Ti ions. The decrease in X-ray density can be ascribed to the increase in lattice constant of the system [15]. The percentage porosity 'P' of all the samples was also determined using the values of X-ray density and bulk density. The values of porosity are also given in **Table 2**. The large values of porosity may be due to the presence of  $Zn^{2+}$  ions in the system.

The average crystal size of all the samples was calculated using the Scherrer's formula given by,

$$t = \frac{0.9\lambda}{\beta \cos\theta}$$

The most intense peak (311) of the XRD patterns was used to determine particle size of the samples. The values of particle size obtained from XRD data are given in **Table 2**.

The distance between magnetic ions that is hopping length at tetrahedral (A) site and octahedral [B] site for all the composition x was calculated in this investigation. The hopping length in ferrite can be calculated for the A-site (tetrahedral) and B-site (octahedral) using the following relations:

$$L_A = a \sqrt{3} / 4 \quad \text{and} \quad L_B = a \sqrt{2} / 4$$

It is observed from table that both hopping length at tetrahedral (A) site  $L_A$  and octahedral [B] site  $L_B$  increases with increasing composition x. The observed behavior of hopping length  $L_A$  and  $L_B$  is attributed to increase in lattice parameter with zinc and titanium composition x as shown in the **Fig. 4**.

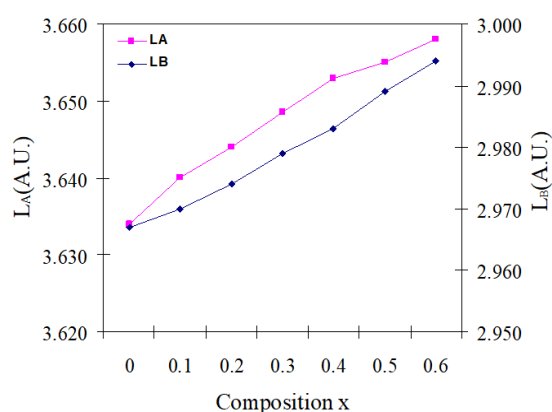


**Fig. 4:** Hopping length in octahedral ' $L_A$ ' and Tetrahedral ' $L_B$ ' sites with Zn-Ti content ' $x$ ' of the system  $MgZn_xTi_xFe_{2-2x}O_4$

The hopping length in ferrite is the distance between magnetic ions, and it influences the physical properties of the ferrite system. The values of hopping length  $L_A$  and  $L_B$  are given in the following **Table 3**.

**Table 3:** Hopping length tetrahedral and octahedral sites ( $L_A$ ,  $L_B$ ), of the  $MgZn_xTi_xFe_{2-2x}O_4$  system

Comp. x	Hopping length (Å)	
	$L_A$	$L_B$
0.0	3.634	2.967
0.1	3.647	2.978
0.2	3.649	2.979
0.3	3.651	2.981
0.4	3.653	2.983
0.5	3.653	2.983
0.6	3.656	2.985

Using the values of lattice constant ' $a$ ' (A.U.) and oxygen positional parameter ' $u$ ', the values of tetrahedral and octahedral bond length ( $d_{AX}$ ) and ( $d_{BX}$ ), shared tetrahedral and octahedral edge can be calculated using the following relations.

$$d_{AX} = a \sqrt{3} (u-1/4)$$

$$d_{BX} = a [3u^2 - (11/4)u + 43/64]^{1/2}$$

$$d_{AXE} = a \sqrt{2} (2u-1/2)$$

$$d_{BXE} = a \sqrt{2} (1-2u)$$

$$d_{BXEU} = a [4u^2 - 3u + (11/16)]^{1/2}$$

The calculated values of all shared tetrahedral and octahedral edge are listed in the following **Table 4**.

**Table 4:** Tetrahedral bond ( $d_{Ax}$ ), octahedral bond ( $d_{Bx}$ ), tetra edge ( $d_{AXE}$ ), octra edge ( $d_{BXE}$ ) of the system  $MgZn_xTi_xFe_{2-2x}O_4$

Com. x	$d_{Ax}$ (Å)	$d_{Bx}$ (Å)	Tetra Edge $d_{AXE}$ (Å)	Octa Edge $d_{BXE}$ (Å)
0.0	1.817	2.097	3.086	2.849
0.1	1.823	2.104	3.097	2.859
0.2	1.824	2.105	3.099	2.860
0.3	1.825	2.106	3.100	2.861
0.4	1.826	2.108	3.102	2.863
0.5	1.826	2.108	3.102	2.864
0.6	1.828	2.109	3.105	2.866

### 3.2. Infrared Studies

The infrared spectra of the present series  $MgZn_xTi_xFe_{2-2x}O_4$  recorded at room temperature for typical samples  $x = 0.2, 0.3, 0.4$ . The spectra have been used to identify the band positions. Two prominent bands are seen in the IR spectra. The high frequency band  $\nu_1$  is seen to be in the range 592 to 620  $cm^{-1}$  and the lower frequency band  $\nu_2$  is in the range 427 to 425  $cm^{-1}$ . Waldron and Hafner have studied the vibrational spectra of the ferrites [16]. According to him the high frequency band  $\nu_1$  is associated with the intrinsic vibration of the tetrahedral complexes and the low frequency band  $\nu_2$  is associated with the intrinsic vibrations of octahedral complexes. The values of absorption bands  $\nu_1$  and  $\nu_2$  and force constant  $K_o$  and  $K_t$  are given in **Table 5**.

The difference in the values of band positions is due to the differences in  $Fe^{3+}-O^{2-}$  distances for octahedral and tetrahedral sites. Our results on IR studies are similar to the literature reports. The IR spectroscopy was used to determine the local symmetry in crystalline and non-crystalline solids

Infrared (IR) spectroscopy is a method that can be used to study ferrites. Using the values of band frequency  $\nu_1$  and  $\nu_2$ , the force constant  $K_t$  and  $K_o$  corresponding to tetrahedral (A) and octahedral [B] site were calculated and the values are given in **Table 5**.

**Table 5:** Vibrational band frequencies  $\nu_1$  and  $\nu_2$  and force constant ' $K_t$ ' and ' $K_o$ ' of the  $MgZn_xTi_xFe_{2-2x}O_4$  system

x	$\nu_1$ $cm^{-1}$	$\nu_2$ $cm^{-1}$	$K_t \times 10^5$ dynes/cm	$K_o \times 10^5$ dynes/cm	$\theta_D$ (K)
0.2	583.2	439.6	1.312	1.022	735
0.3	585.7	442.7	1.137	1.010	739
0.4	590.9	443.1	1.465	1.042	743

The table 5 reports that the average values of the band positions were used to calculate the Debye temperature  $\theta_D$ . The Debye temperature was investigated by using the following equation,

$$\theta_D = \lambda \times C \times \nu_{av}$$

The values of Debye temperature are also given in the **Table 5**. The Debye temperature is a temperature that represents the highest normal mode of vibration in a crystal. It's a measure of the cutoff frequency and is used to correlate elastic properties. From table 5, it is clear from



the values are given in the table that, the Debye temperature increases with Zn, Ti concentration 'x'. The values of Vibrational band frequencies  $\nu_1$  and  $\nu_2$  and force constant 'K<sub>t</sub>' and 'K<sub>o</sub>' of the system increases with the concentration x.

#### 4. Conclusions

The experimental results on the structural properties and Infrared studies of the investigated system  $MgZn_xTi_xFe_{2-2x}O_4$  led us to draw following conclusions.

The analysis of X-ray diffraction patterns revealed the formation of single-phase cubic spinel structure of all the samples under investigation. The lattice constant increases with Zn, Ti concentration 'x'. The X-ray density decreases with increase in Zn, Ti concentration 'x'. The values of bulk density increase with Ti and Zn ions and porosity values varies in between 36% - 48%. The average particle size of all sample showed good agreement with the reported data and the values of hopping length, tetrahedral and octahedral bond length ( $d_{Ax}$ ) and ( $d_{Bx}$ ), shared tetrahedral and octahedral edge shows same behavior that of lattice constant. shows same behavior that of lattice constant. Two prominent absorption bands are seen in the Infrared (IR) spectra, which is the characteristic feature of spinel ferrite. The study of the present series is recorded at room temperature shows two prominent band position associated with intrinsic vibration of the tetrahedral complexes for high frequency and for low frequency bands associated with octahedral complexes. Debye temperature obtained from infrared spectrum data increases with composition 'x'.

#### 5. References

- [1]. M.L.S. Teo, L.B. Kong, Z.W. Li, G.Q. Lin, Y.B. Gan, *J. Alloys Compd.* 459 (2008) 567.
- [2]. L.B. Kong, M.L.S. Teo, Z.W. Li, G.Q. Lin, Y.B. Gan, *J. Alloys Compd.* 459 (2008) 576.
- [3]. J. Kim, C. Ham, *Mater. Res. Bull.* 44 (2009) 633.
- [4]. K. Sadhana, K. Praveena, S. Bharadwaj, S. R. Murthy, *J. Alloys Compd.* 472 (2009) 484.
- [5]. S. Maensiri, C. Masingboon, B. Boonchom, S. Seraphin, *Scripta Mater.* 56 (2007) 797.
- [6]. P.A. Jadhav, R.S. Devan, Y.D. Kolekar, B.K. Chougule, *J. Phys. Chem. Sol.* 70 (2009) 396.
- [7]. F. Scholl, K. Binder, *Z. Phys. B.* 39 (1980) 239
- [8]. U. Lima, M. Nasara, R. Nasara, M. Rezende, J. Araujo, *Mater. Sci. Eng. B* 151 (2009) 238.
- [9]. M. Dimri, A. Verma, S. Kashyap, D. Dube, O. Thakur, C. Prakash, *Mater. Sci. Eng.* 133(2006) 42.
- [10]. M.A. Gabal, *J. Magn. Magn. Mater.* 321 (2009) 3144.
- [11]. Y. Abbas, M. A. Ahed, M. A. Semary, *J. Mater. Sci.* 18 (1983) 2890.
- [12]. H. H. Joshi, R. G. Kulkarni, *J. Mater. Sci.* 21 (1986) 2138
- [13]. Dinesh Varshney, Kavita Verma, Ashwini Kumar, *J. Mol. Struct.* (2011) 447.
- [14]. M. Manjurul Haque, M. Huq, M.A. Hakim, *J. Phys. D Appl. Phys.* 41 (2008) 055007. (10pp).
- [15]. Hussein A. Dawoud, Samy K. Shaat, H. Dawoud, *J. Al-Aqsa Univ.* 10 (S.E) (2006) 247.
- [16]. N.W. Grimes *Spectrochimica Acta Part A: Molecular Spectroscopy*, 28, (11)1972, 2217-2225.